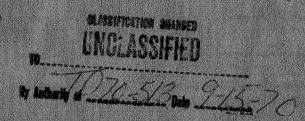
## NASA TECHNICAL MEMORANDUM



NASA TM X-1029

(CODE)
(NASA CR OR TMX OR AD NUMBER)
(CATEGORY)

Declessified by authority of NASA Classification Change Notices No.



AERODYNAMIC CHARACTERISTICS OF A BLUNT, HALF-CONE ENTRY CONFIGURATION, WITH HORIZONTAL LANDING CAPABILITY

by Joseph H. Kemp, Jr., George H. Holdaway, and Thomas E. Polek

Ames Research Center Moffett Field, Calif.

NATIONAL AERONAUTICS AND SPACE ADMINISTRATION . WASHINGTON, D. C. . OCTOBER 1964

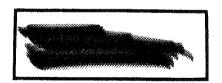
# CASE FILE COPY



# AERODYNAMIC CHARACTERISTICS OF A BLUNT, HALF-CONE ENTRY CONFIGURATION, WITH HORIZONTAL LANDING CAPABILITY

By Joseph H. Kemp, Jr., George H. Holdaway, and Thomas E. Polek

Ames Research Center Moffett Field, Calif.





NATIONAL AERONAUTICS AND SPACE ADMINISTRATION





### AERODYNAMIC CHARACTERISTICS OF A BLUNT, HALF-CONE ENTRY

CONFIGURATION, WITH HORIZONTAL LANDING CAPABILITY\*

By Joseph H. Kemp, Jr., George H. Holdaway, and Thomas E. Polek

Ames Research Center Moffett Field, Calif.

### SUMMARY

17/65

An investigation was conducted in the Ames 14-inch helium tunnel to determine the hypersonic aerodynamic characteristics of an entry configuration consisting of approximately half of a blunted cone having a semivertex angle of 30° and a faired afterbody. The faired afterbody was added to the basic entry configuration to provide a horizontal landing capability. The tests were conducted using helium as a test gas at Mach numbers of 10.7 and 21.2 with Reynolds numbers of 800,000 and 1,200,000, respectively, based on the length of the unmodified body.

The results indicate that the modified configuration has a higher lift-drag ratio and greater stability, about all three axes, then does the unmodified M-l configuration. The configuration was found to be trimmed and stable without control deflections at a maximum  $\ L/D$  of 0.65 for a moment reference center located at 5 percent of the body length directly forward of the center of volume.

Data presented in the appendix show that the configuration has subsonic aerodynamic characteristics which indicate a horizontal landing capability comparable to the M-2 configuration.

### INTRODUCTION

The advantages of a lifting entry trajectory over a ballistic entry trajectory, as described in reference 1, are well known. One shape which has received considerable attention for lifting entry consists of approximately half of a blunted cone with semivertex angle of 30°. This configuration commonly known as the Ames M-1 has been investigated from subsonic to hypersonic speeds as indicated in references 2 through 6. From these investigations this configuration was found to be suitable for hypersonic speeds; however, like most entry configurations it is incapable of horizontal landing and thus requires some auxiliary equipment, such as a parachute, for safe landing.

In an unpublished investigation, George G. Edwards and George C. Kenyon at Ames Research Center considered variations to the basic M-1 configuration necessary to permit a horizontal landing. Some of the results from this

Unclassified



investigation are presented in the appendix. These results show that the addition of a faired afterbody to the basic M-l configuration provides it with subsonic characteristics comparable to the Ames M-2 which has been flight tested recently at the Flight Research Center at Edwards and has been shown to have a horizontal landing capability.

The present investigation was undertaken to see if the modification to the M-l caused any significant changes in the aerodynamic characteristics at hypersonic speeds, which might affect its use as an entry configuration. This modified configuration is hereafter referred to as the M-l-L.

### NOTATION

All force coefficients are referred to the stability axes, and the moment coefficients are referred to the body axes with the moment reference center located as shown in figure 1. Also shown in figure 1 are the reference axes for  $\alpha$  and  $\beta$ .

| A                               | base area of basic M-1, 0.5686d <sup>2</sup>                             |  |  |  |  |  |
|---------------------------------|--|--|--|--|--|--|
| $C_{\mathrm{D}}$                | drag coefficient, $\frac{d\text{rag}}{q_{\infty}A}$                      |  |  |  |  |  |
| $\mathtt{C}_{\mathtt{L}}$       | lift coefficient, $\frac{\text{lift}}{q_{\infty}A}$                      |  |  |  |  |  |
| Cl                              | rolling-moment coefficient, $\frac{\text{rolling moment}}{q_{\infty}Ad}$ |  |  |  |  |  |
| $C_{\mathrm{m}}$                | pitching-moment coefficient, pitching moment $q_{\infty} ^{\text{Al}}$   |  |  |  |  |  |
| $C_n$                           | yawing-moment coefficient, $\frac{\text{yawing moment}}{q_{\infty}Ad}$   |  |  |  |  |  |
| $\mathtt{C}^{\underline{Y}}$    | side-force coefficient, side force $q_{\infty}A$                         |  |  |  |  |  |
| c.g., ref                       | moment reference center (see figs. 1 and 8)                              |  |  |  |  |  |
| đ                               | base diameter of M-1   |  |  |  |  |  |
| 7                               | length of M-1  |  |  |  |  |  |
| $\frac{\mathbf{L}}{\mathbf{D}}$ | lift-drag ratio  |  |  |  |  |  |
| M                               | Mach number  |  |  |  |  |  |
| $q_{\infty}$                    | free-stream dynamic pressure   |  |  |  |  |  |







|          | r          | radius of curvature of lower surface of model  |  |  |  |  |  |  |  |  |
|----------|------------|--|--|--|--|--|--|--|--|--|
|          | x t        | coordinate measurement parallel to conical center line of model  |  |  |  |  |  |  |  |  |
|          | X          | coordinate measurement parallel to the upper surface of the model forebody   |  |  |  |  |  |  |  |  |
| 4        | Z          | coordinate measurement perpendicular to the conical center line of the model in the vertical direction  coordinate measurement perpendicular to the upper surface of the model |  |  |  |  |  |  |  |  |
| <b>€</b> | Z          |  |  |  |  |  |  |  |  |  |
|          | α          | angle of attack (measured with respect to flat upper surface of the forebody)  |  |  |  |  |  |  |  |  |
|          | β          | angle of sideslip  |  |  |  |  |  |  |  |  |
|          | Subscripts |  |  |  |  |  |  |  |  |  |
|          | α          | derivative with respect to angle of attack   |  |  |  |  |  |  |  |  |
|          | β          | derivative with respect to angle of sideslip   |  |  |  |  |  |  |  |  |
|          | trim       | value at trim condition  |  |  |  |  |  |  |  |  |
|          | max        | maximum value  |  |  |  |  |  |  |  |  |

### APPARATUS AND MODELS

The tests were conducted in the Ames 14-inch helium tunnel. This tunnel, shown schematically in figure 2 and described in detail in reference 6, is of the blowdown type and operates at nominal Mach numbers of 11, 17, and 21 utilizing helium as the test gas.

Forces and moments were measured by a six-component strain-gage balance mounted on a model support system capable of providing angle variations of  $\pm 14^{\circ}$ . Bent stings were used to extend the angle-of-attack range and obtain sideslip.

The dimensions of the test models are shown in figure 1. The basic configuration consists of a forebody which is approximately half of a blunted cone with a semiapex angle of 30° and an afterbody formed by extending the conical surface with a faired body of revolution and extending the upper surface with a ruled surface, in which the generating line is perpendicular to the vertical plane of the body, so that the base area is decreased. Vertical fins have been added to the upper surface of the afterbody slightly





inboard of the outer edge for subsonic stability and control. Two models were constructed, one shown in figure 3(a) had the balance cavity at a  $30^{\circ}$  angle relative to the upper forebody surface, and the second shown in figure 3(b) had the balance cavity parallel to this surface.

### TESTS AND PROCEDURES

The tests were conducted at free-stream Mach numbers of 10.7 and 21.2 and Reynolds numbers based on the length of the unmodified M-1 of 800,000 and 1,200,000, respectively.

The force coefficients are referred to the stability axes, and the moment coefficients are referred to the body axes. All coefficients are referred to the base area and moment reference of the M-l as used in references 2 through 6. Similarly, the pitching-moment coefficients are referred to the M-l body length and the yawing- and rolling-moment coefficients to the M-l base diameter.

The force and moment coefficients include the contribution of the forces on the body base as they existed during the tests. Base pressures were measured and from these it was found that the total contributions of the base forces to  $C_{\rm L}$  and  $C_{\rm D}$  were less than 0.003 and 0.010, respectively.

The theoretical estimates of the aerodynamic coefficients presented in the figures are based on modified Newtonian impact theory. These estimates were made using the total pressure coefficient downstream of a normal shock wave in helium, 1.76, rather than the unmodified Newtonian value of 2.00.

### PRECISION

The estimated maximum errors due to contributions of measured stream angularities, instrumentation, and/or data-recording errors are listed in the following table.

| M    | $\mathtt{C}_{\mathbf{L}}$ | $\mathtt{C}_{\mathrm{D}}$ | $\mathrm{C}^{\mathrm{X}}$ | CZ     | $c_{\mathrm{m}}$ | $c_n$ | α    | β    |
|------|---------------------------|---------------------------|---------------------------|--------|------------------|-------|------|------|
| 10.7 | 0.010                     | 0,008                     | 0.006                     | 0.0029 | 0.013            | 0.014 | 0.20 | 0.20 |
| 21.2 | .017                      | .014                      | .009                      | .0048  | .022             | .023  | ,2°  | .20  |

The effect of the uncertainty in the dynamic pressure is not included in the above values; however, it is less than 1 percent for Mach number 10.7 and 1.5 percent for Mach number 21.2.





### RESULTS AND DISCUSSION

The aerodynamic characteristics of the M-1-L configuration are presented in figures 4, 5, and 6. These characteristics are compared with those for the M-1 in figure 7, and an analysis of the effect of the location of the moment reference center on trim characteristics is shown in figure 8.

The aerodynamic characteristics of the M-1-L were very nearly the same for the two Mach numbers. The maximum L/D was about 0.65 and occurred near zero angle of attack. The trim angle of attack is about  $-14^{\rm O}$  with an L/D of about 0.4 for the moment reference originally used with the M-1. The theoretical estimates shown in figures 4 and 5 are in relatively good agreement with the experimental results.

The M-l-L configuration was laterally and directionally stable with only relatively small variations in stability over the angle-of-attack range from -14° to +14° as shown in figure 6(a). These results were generally determined from two-point slopes of data obtained at sideslip angles of 0° and 7°. The slopes at zero angle of attack and the linearity of the data at small angles of sideslip were verified by results obtained for  $\beta$  = -14° to +14° as shown in figure 6(b).

Additional data presented in figures 5 and 6(b) show the variation of the aerodynamic characteristics of the M-1-L with and without vertical fins. From these data it is apparent that the effect of the vertical fins on the aerodynamic coefficients at hypersonic speeds is very small.

As was expected, the addition of the afterbody to the M-l increased the lift, the drag, and the longitudinal and directional stability (see fig. 7). These increases tend to become smaller at negative angles of attack where the afterbody becomes shaded. An increase in the  $\rm L/D$  also occurred which was nearly constant over the angle-of-attack range shown. Also noted is a large negative shift in the trim point which is due to the additional lift of the afterbody creating a negative moment.

### Moment-Reference Effect on Trim Conditions

The moment-center location initially chosen for the M-1-L was the same as that for the basic M-1. As noted, this location does not provide trim without control deflection at the maximum L/D generally desired. Since trim at or near maximum L/D would require a change in the moment-reference center, an analysis was made to indicate the moment-center locations required to provide trim at various angles of attack for a given stability. These results are presented in figure 8. Imposed on a sketch of the M-1-L are lines of constant trim angle of attack and constant stability at trim. The intersection of the two lines indicate the moment-center location required for the trim condition indicated. The trim angles shown will provide an L/D of 0.5 or greater. It is apparent that the configuration is stable and





trimmed for a number of center-of-gravity locations. One condition for which the configuration is trimmed at  $0^{\circ}$  angle of attack (maximum L/D) is with the center of gravity located about 5 percent of the body length directly forward of the center of volume.

The quadrant labeled "off trim instability area" represents moment-center locations for which a secondary unstable trim point occurs for some angle of attack greater than -15°.

A check was also made on the lateral-directional stability characteristics with variations in the moment-reference center and it was found that the configuration is laterally and directionally stable for any moment-center location which provides longitudinal stability.

### CONCLUDING REMARKS

A configuration, basically the Ames M-l, modified to have a horizontal landing capability, was investigated at Mach numbers 10.7 and 21.2 in helium. For these Mach numbers the modifications increased the lift, drag, lift-drag ratio, and stability. The configuration is statically stable about all three axes and is trimmed without control deflections at a maximum L/D of 0.65 for a moment-reference center located 5 percent of the body length directly forward of the center of volume.

From data presented in the appendix it is apparent that the M-l-L should have a horizontal landing capability comparable to the M-2.

Ames Research Center
National Aeronautics and Space Administration
Moffett Field, Calif., July 21, 1964





### COMPARISON OF THE M-1-L WITH THE M-2 AT SUBSONIC SPEED

Previously unpublished subsonic data for the M-1-L which was obtained by Edwards and Kenyon in the Ames 12-foot wind tunnel are presented in figures 9 and 10. Here aerodynamic characteristics for the M-1-L are compared with the characteristics for the M-2 as given in references 7 and 8. For ease of comparison, the angles of attack for both models are measured relative to the lower cone meridian lines of the models.

The aerodynamic coefficients are referred to the body plan-form area, with pitching moments referenced to the maximum body lengths parallel to the conical center lines. The reference lengths for yawing and rolling moments are the spans of the body bases. Reynolds numbers shown are also referred to the maximum body lengths parallel to the conical center lines.

These results indicate that the longitudinal characteristics of the M-1-L are very nearly the same as those of the M-2. The only notable difference is in the angle of trim. This difference would be reduced by a rearward shift in the moment-reference center.

The lateral and directional stability data indicate that the M-1-L is stable although not as stable as the M-2. From these data it is concluded that the M-1-L is probably capable of horizontal landing at reasonable touchdown speeds.





### REFERENCES

- 1. Koelle, Heinz Hermann, ed.: Handbook of Astronautical Engineering, Ch. 10, Atmospheric Entry by Carl Gazley, Jr. McGraw-Hill Book Company, Inc., N. Y.. 1961.
- 2. Eggers, Alfred J., Jr., and Wong, Thomas J.: Re-entry and Recovery of Near-Earth Satellites, With Particular Attention to a Manned Vehicle. NASA MEMO 10-2-58A, 1958.
- 3. Holtzclaw, Ralph W.: Static Stability and Control Characteristics of a Half-Cone Entry Configuration at Mach Numbers 2.2 to 0.7.

  NASA TM X-649, 1962.
- 4. Sarabia, Michael F.: Aerodynamic Characteristics of a Blunt Half-Cone Entry Configuration at Mach Numbers From 3 to 6. NASA TM X-393, 1960.
- 5. Holdaway, George H., Polek, Thomas E., and Kemp, Joseph H., Jr.:
  Aerodynamic Characteristics of a Blunt Half-Cone Entry Configuration at
  Mach Numbers of 5.2, 7.4, and 10.4. NASA TM X-782, 1963.
- 6. McDevitt, John B., and Mellenthin, Jack A.: Characteristics of a Blunt Half-Cone Entry Configuration at Mach Numbers From 10.9 to 21.2 in Helium. NASA TM X-655, 1962.
- 7. Kenyon, George C., and Sutton, Fred B.: The Longitudinal Aerodynamic Characteristics of a Re-entry Configuration Based on a Blunt 13° Half-Cone at Mach Numbers to 0.92. NASA TM X-571, 1961.
- 8. Kenyon, George C.: The Lateral and Directional Aerodynamic Characteristics of a Re-entry Configuration Based on a Blunt 13° Half-Cone at Mach Numbers to 0.92. NASA TM X-583, 1961.



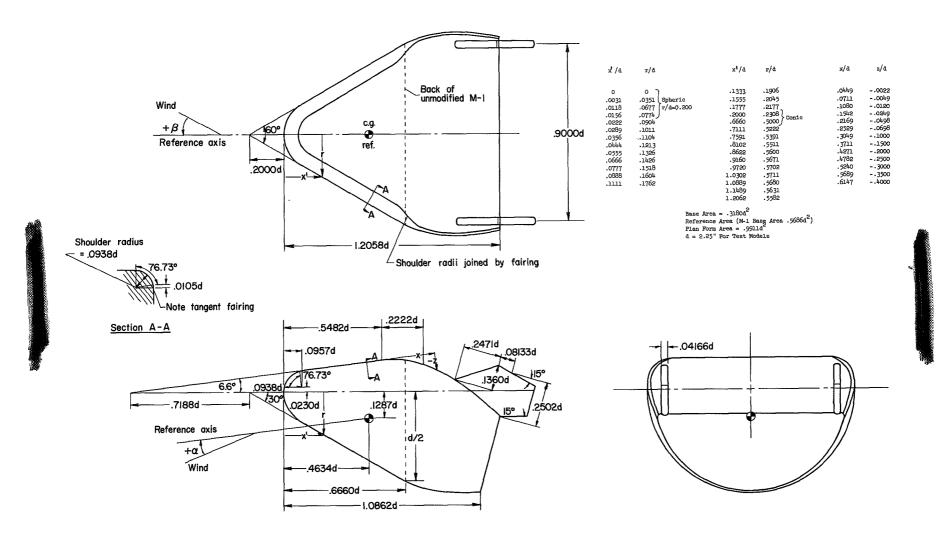
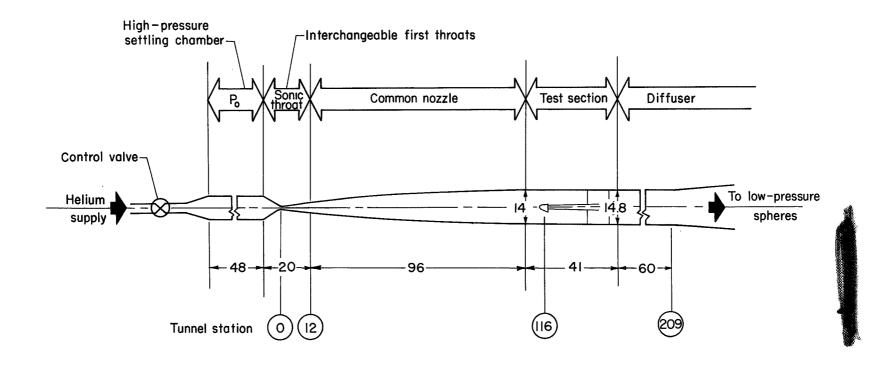


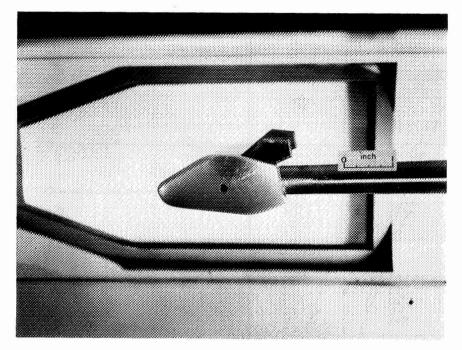
Figure 1.- Dimensions of the test models.



Note: All dimensions in inches

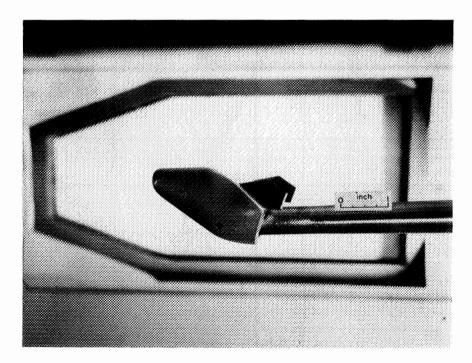
Figure 2.- Sketch of the Ames 14-inch helium tunnel.





(a)  $-30^{\circ}$  model.

A-32060

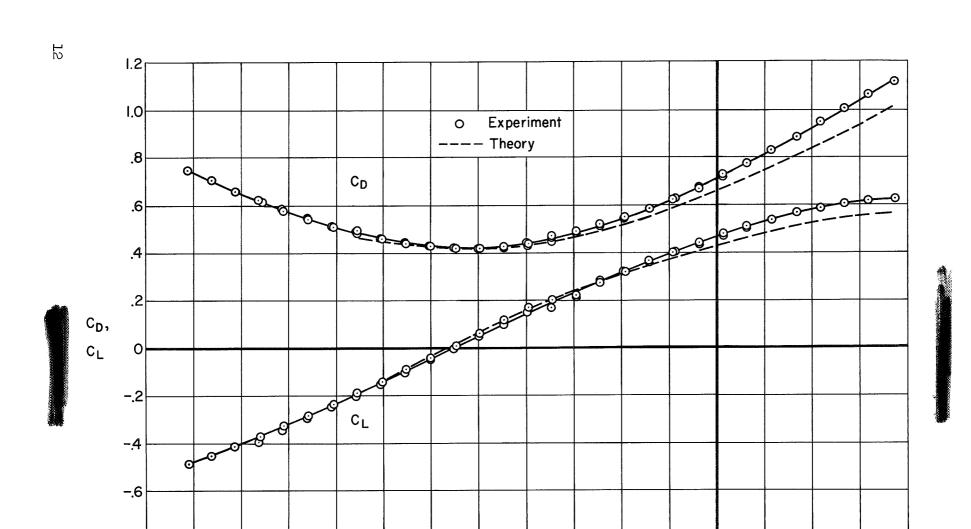


(b) OO model.

A-32061

Figure 3.- Photographs of the test models.





(a)  $C_{
m D}$  and  $C_{
m L}$ 

 $\alpha$ , deg

-12

-20 -16

-24

-28

-32

-40

-36

12

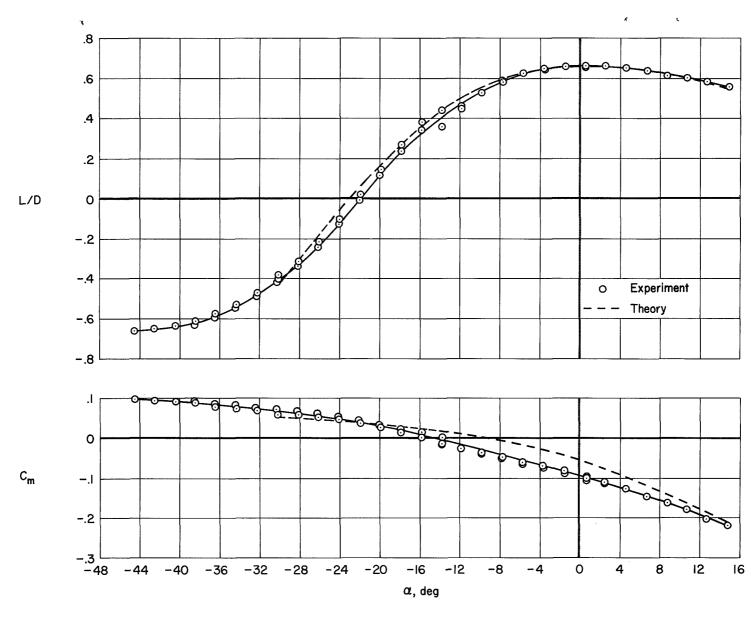
8

0

4

16

Figure 4.- Longitudinal aerodynamic characteristics of the M-1-L at M =10.7.



(b) L/D and  $C_{\rm m}$ 

Figure 4.- Concluded.

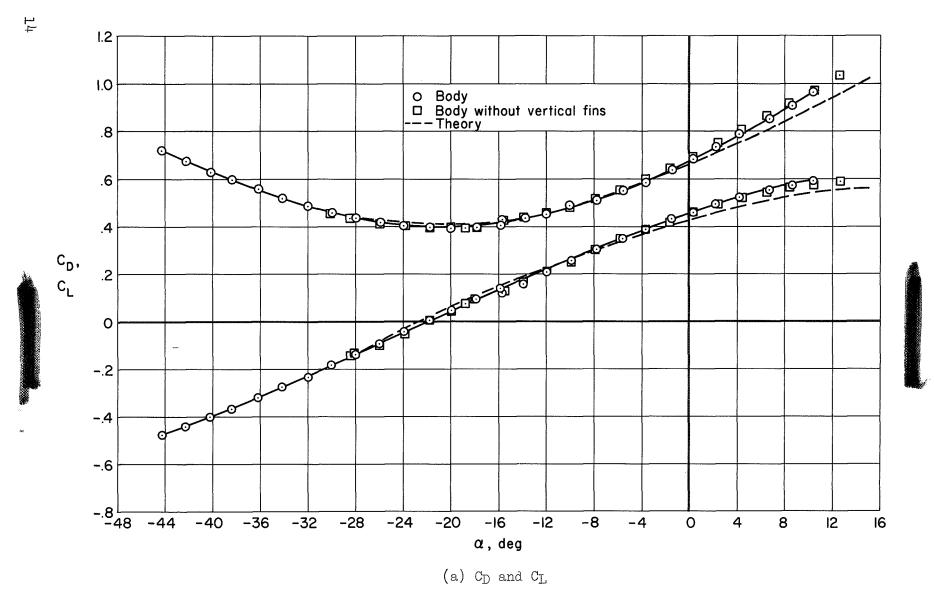
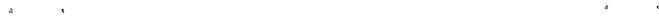
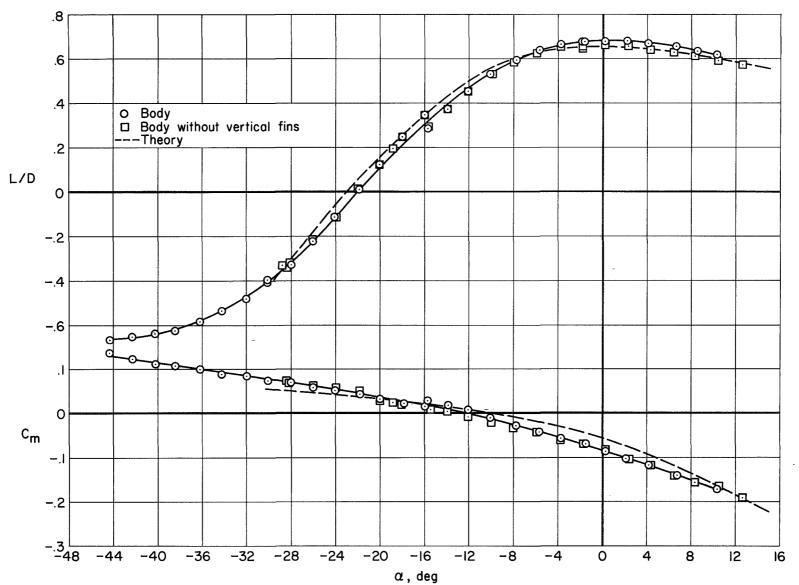


Figure 5.- Longitudinal aerodynamic characteristics of the M-1-L at M=21.2.





(b) L/D and  $C_{\rm m}$ 

Figure 5.- Concluded.



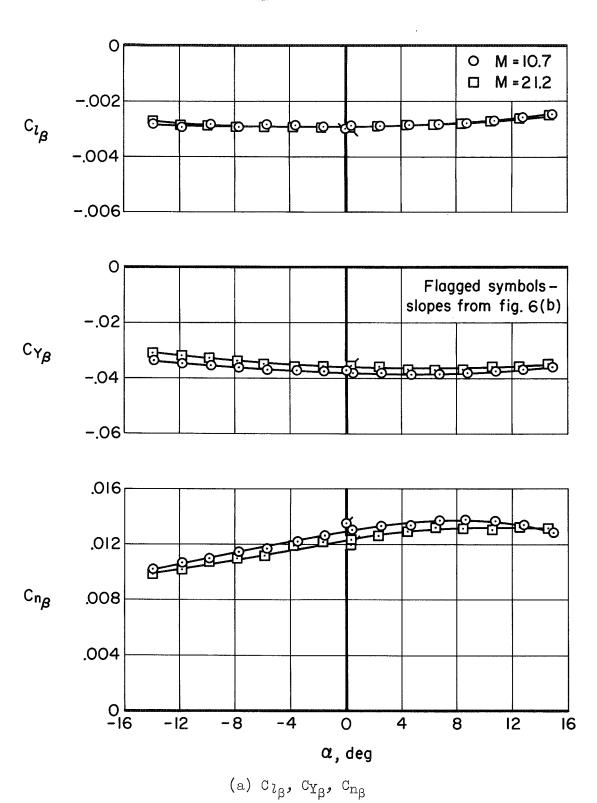
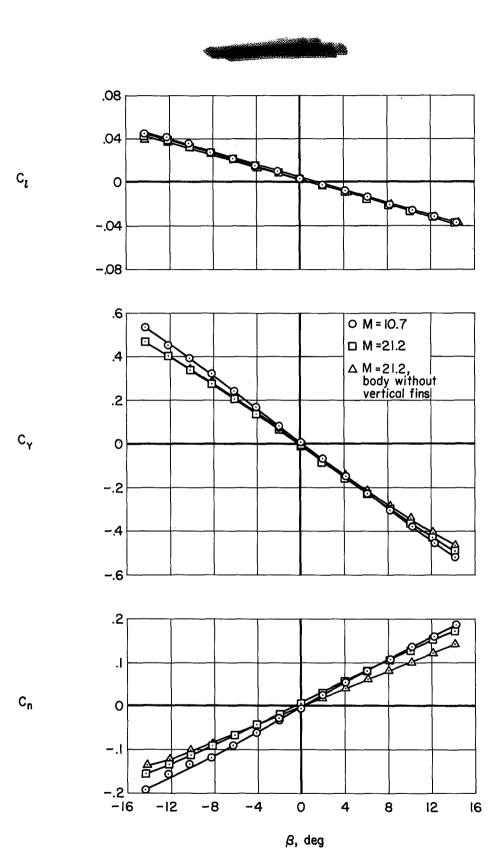


Figure 6.- Lateral and directional characteristics of the M-1-L at M = 10.7 and 21.2.





(b)  $C_l$ ,  $C_Y$ ,  $C_n$ 

Figure 6.- Concluded.

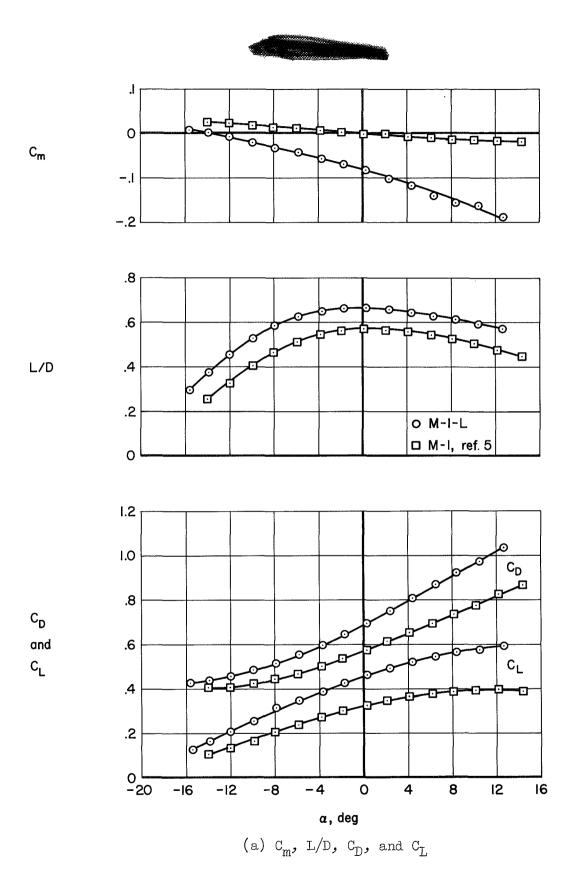
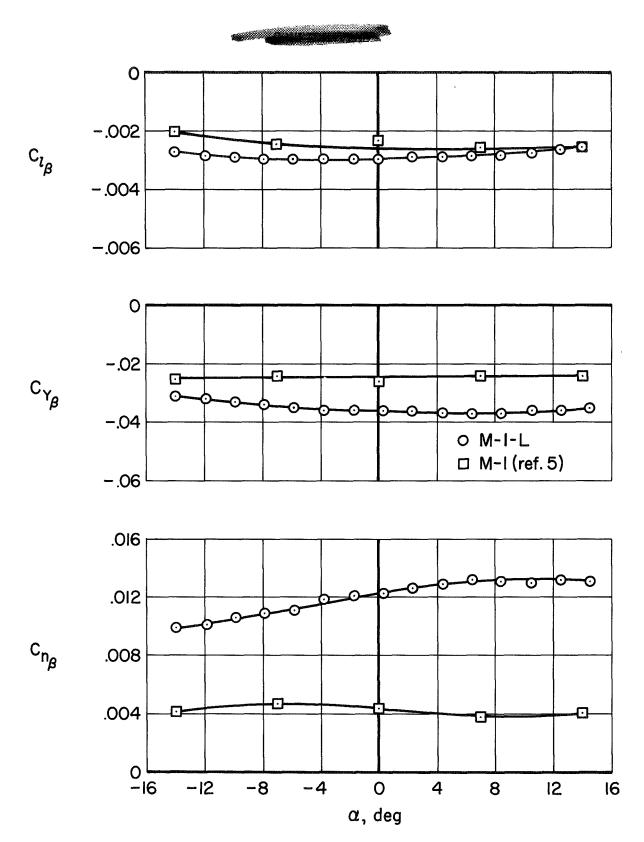


Figure 7.- Comparison of the aerodynamic characteristics of the M-1 and the M-1-L at M=21.2.



(b)  $C_{1\beta}$ ,  $C_{Y\beta}$ , and  $C_{n\beta}$  Figure 7.- Concluded.

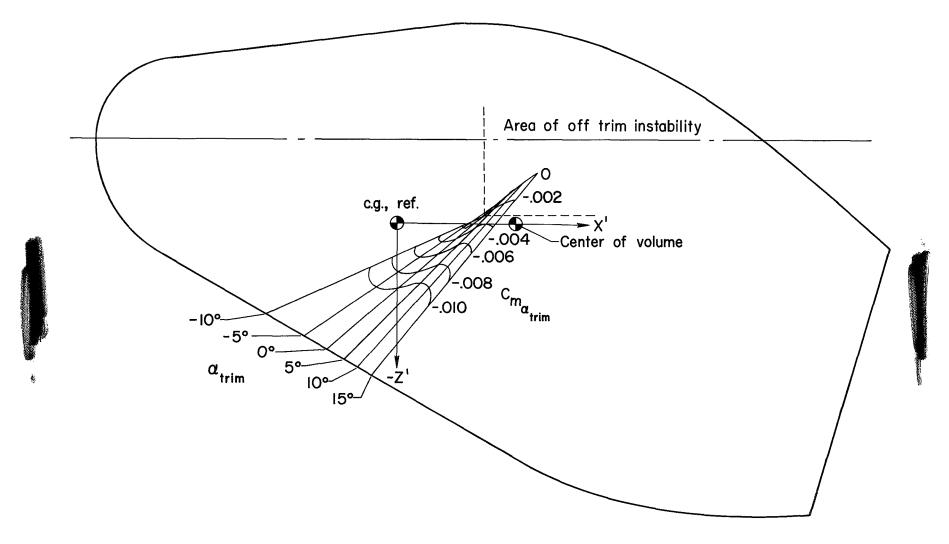


Figure 8.- Moment-center locations for various trim conditions at Mach number 10.7.

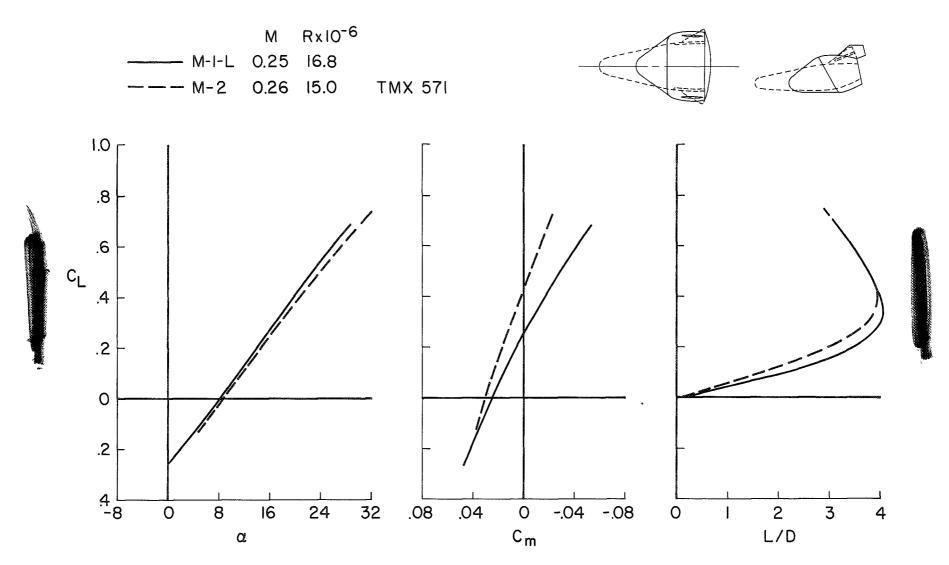


Figure 9.- Comparison of longitudinal characteristics of M-1-L and M-2.

Figure 10.- Comparison of lateral-directional characteristics of M-1-L and M-1.

"The aeronautical and space activities of the United States shall be conducted so as to contribute... to the expansion of human knowledge of phenomena in the atmosphere and space. The Administration shall provide for the widest practicable and appropriate dissemination of information concerning its activities and the results thereof."

-NATIONAL AFRONAUTICS AND SPACE ACT OF 1958

### NASA SCIENTIFIC AND TECHNICAL PUBLICATIONS

TECHNICAL REPORTS: Scientific and technical information considered important, complete, and a lasting contribution to existing knowledge.

TECHNICAL NOTES: Information less broad in scope but nevertheless of importance as a contribution to existing knowledge.

TECHNICAL MEMORANDUMS: Information receiving limited distribution because of preliminary data, security classification, or other reasons.

CONTRACTOR REPORTS: Technical information generated in connection with a NASA contract or grant and released under NASA auspices.

TECHNICAL TRANSLATIONS: Information published in a foreign language considered to merit NASA distribution in English.

TECHNICAL REPRINTS: Information derived from NASA activities and initially published in the form of journal articles.

SPECIAL PUBLICATIONS: Information derived from or of value to NASA activities but not necessarily reporting the results of individual NASA-programmed scientific efforts. Publications include conference proceedings, monographs, data compilations, handbooks, sourcebooks, and special bibliographies.

Details on the availability of these publications may be obtained from:

SCIENTIFIC AND TECHNICAL INFORMATION DIVISION
NATIONAL AERONAUTICS AND SPACE ADMINISTRATION

Washington, D.C. 20546